Geochemistry Geophysics Geosystems G3

Article
Volume 14, Number 9
5 September 2013
doi: 10.1002/ggge.20215
ISSN: 1525-2027

Published by AGU and the Geochemical Society

Trace metal and carbon isotopic variations in cave dripwater and stalagmite geochemistry from northern Borneo

Judson W. Partin
School of Earth and Atmospheric Sciences, Georgia Institute of Technology, Atlanta, Georgia, USA

Now at Institute for Geophysics, Jackson School of Geosciences, J.J. Pickle Research Campus, University of Texas at Austin, Building 196, 10100 Burnet Road (R2200), Austin, Texas, 78758-4445, USA (jpartin@ig.utexas.edu)

Kim M. Cobb
School of Earth and Atmospheric Sciences, Georgia Institute of Technology, Atlanta, Georgia, USA

Jess F. Adkins
Division of Geological and Planetary Sciences, California Institute of Technology, Pasadena, California, USA

Andrew A. Tuen
Institute of Biodiversity and Environmental Conservation, Universiti Malaysia Sarawak, Sarawak, Malaysia

Brian Clark
Gunung Mulu National Park, Sarawak, Malaysia

[1] We investigate stalagmite trace metal ratios and carbon isotopic composition ($\delta^{13}C$) as potential paleoclimate proxies by comparing cave dripwaters, stalagmites, and bedrock composition from Gunung Mulu and Gunung Buda National Parks in northern Borneo, a tropical rainforest karst site. Three year long, biweekly time series of dripwater Mg/Ca, Sr/Ca, and $\delta^{13}C$ from several drips at our site are not correlated with rainfall variability, indicative of a relatively weak relationship between hydroclimate and dripwater geochemistry at our site. However, combining all of the dripwater geochemical data gathered over four field trips to our site ($N > 300$ samples), we find that drips with highly variable Mg[Sr]/Ca have relatively invariable $\delta^{18}O$ values close to the mean. We hypothesize that increased residence times translate into reduced variance in dripwater $\delta^{18}O$ through mixing in the epikarst as well as increased Mg[Sr]/Ca values through increased calcite precipitation in the epikarst. Mg/Ca, Sr/Ca, and $\delta^{13}C$ time series from three overlapping stalagmites that grew over the last 27 kyrs are characterized by strong centennial-scale variations, and bear little resemblance to previously published, well-reproduced $\delta^{18}O$ time series from the same stalagmites. The only shared signal among the three stalagmites' geochemical time series is a relative decrease of 1‰ in $\delta^{13}C$ from the Last Glacial Maximum to the Holocene, consistent with a transition from savannah (C4) to rainforest (C3) conditions documented in nearby records. Taken together, our study indicates that stalagmite Mg[Sr]/Ca ratios are poor indicators of hydroclimate conditions at our site, while stalagmite $\delta^{13}C$ exhibits some reproducible signals on glacial-interglacial timescales.

Components: 11,578 words, 12 figures, 7 tables.

Keywords: stalagmite; speleothem; stable isotopic composition; trace metal ratio; Western Pacific warm pool; paleoclimate

Index Terms: 1065 Major and trace element geochemistry: Geochemistry; 1041 Stable isotope geochemistry: Geochemistry; 1090 Field relationships: Geochemistry; 0454 Isotopic composition and chemistry: Biogeosciences; 0473 Paleoclimatology and paleoceanography: Biogeosciences; 4870 Stable isotopes: Oceanography: Biological and Chemical; 4900 Paleoceanography: Oceanography: Biological and Chemical; 3690 Field relationships: Mineralogy and Petrology; 8486 Field relationships: Volcanology; 3344 Paleoclimatology: Atmospheric Processes; 3305 Climate change and variability: Atmospheric Processes; 1616 Climate variability: Global Change; 1635 Oceans: Global Change; 3309 Climatology: Global Change; 4215 Climate and interannual variability: Oceanography: General; 4513 Decadal ocean variability: Oceanography: Physical.

Received 11 January 2013; **Revised** 24 June 2013; **Accepted** 30 June 2013; **Published** 5 September 2013.

Partin, J. W., K. M. Cobb, J. F. Adkins, A. A. Tuen, and B. Clark (2013), Trace metal and carbon isotopic variations in cave dripwater and stalagmite geochemistry from northern Borneo, *Geochem. Geophys. Geosyst.*, *14*, 3567–3585, doi:10.1002/ggge.20215.

1. Introduction

[2] Stalagmites are valuable archives of terrestrial paleoclimate because they form in karst systems located around the world, can be absolute-dated, and afford high-resolution reconstructions on glacial-interglacial timescales. Stalagmite oxygen isotopic composition ($\delta^{18}O$) is the primary proxy used for stalagmite paleoclimate reconstructions because it reflects changes in rainfall $\delta^{18}O$ that are related to rainfall amount [*Dansgaard*, 1964; *Rozanski et al*., 1993; *Moerman et al*., 2013], moisture trajectories/histories [*Cruz et al*., 2005; *Cobb et al*., 2007], and in some cases temperature [*Meyer et al*., 2006]. Stalagmite $\delta^{18}O$ records have captured changes in hydrological conditions on glacial-interglacial timescales [*Bar-Matthews et al*., 1997; *Hellstrom et al*., 1998; *Williams et al*., 2005], identified insolation-related changes in orbital-scale hydrology [*Wang et al*., 2001; *Fleitmann et al*., 2003; *Holmgren et al*., 2003; *Cruz et al*., 2005; *Wang et al*., 2006], and have been used to constrain the timing and regional expression of abrupt climate changes [*Bar-Matthews et al*., 1997; *Wang et al*., 2001; *Burns et al*., 2003; *Williams et al*., 2005]. Stalagmite $\delta^{18}O$ records reproduce across multiple samples at a site [*Fleitmann et al*., 2007; *Partin et al*., 2007; *Cheng et al*., 2009; *Griffiths et al*., 2009] and across multiple caves in a given region [*Fleitmann et al*., 2007; *Cheng et al*., 2009; *Cruz et al*., 2009], supporting their interpretation as robust climate archives.

[3] Many studies suggest that the concentrations of trace metals such as Mg^{2+} and Sr^{2+} in stalagmites may vary as a function of hydrological conditions [*Roberts et al*., 1998; *Fairchild et al*., 2000, 2001; *Huang et al*., 2001; *Treble et al*., 2003; *McDermott*, 2004; *McMillan et al*., 2005; *Treble et al*., 2005; *Fairchild et al*., 2006; *Johnson et al*., 2006; *Cruz et al*., 2007; *Sinclair et al*., 2012]. In a mechanism often referred to as "prior calcite precipitation" (PCP), calcium carbonate precipitation/dissolution cycles that take place in the karst upstream of stalagmites fractionate dripwater Mg/Ca, Sr/Ca, and Ba/Ca values [*Roberts et al*., 1998; *Fairchild et al*., 2000, 2001; *Galy et al*., 2002; *Treble et al*., 2003; *Johnson et al*., 2006; *Sinclair*, 2011; *Sinclair et al*., 2012]. During dry times, evaporation and/or CO_2 degassing drive the precipitation of calcite, which discriminates against Mg, Sr, and Ba, thereby continually enriching the dripwater Metal/Ca ratio. Alternative mechanisms for increasing trace metal ratios in karst waters include selective leaching of trace metals from soils and calcium carbonate bedrock [*Fairchild et al*., 2000], changes in temperature that affect the metal distribution coefficients [*Ihlenfeld et al*., 2003], and crystal growth rate changes [*Lorens*, 1981; *Paquette and Reeder*, 1995]. Additionally, in areas with dolomitic limestone, dissolution of this mineral [*Fairchild et al*., 2000] can heavily influence the Mg/Ca ratio of cave dripwaters.

[4] Stalagmite carbon isotopic composition ($\delta^{13}C$) responds to a host of influences including vegetation type [*Dorale et al*., 1998; *Hellstrom et al*., 1998; *Bar-Matthews et al*., 1999; *Genty et al*., 2003], biogenic CO_2 produced in soils [*Frappier et al*., 2002; *Cruz et al*., 2006], and groundwater geochemical processes [*McMillan et al*., 2005; *Fairchild et al*., 2006] some of which are affected by changes in rainfall amount. Most commonly, stalagmite $\delta^{13}C$ has been used as a proxy for C_3 versus C_4 vegetation changes that occur on millennial timescales [*Dorale et al*., 1998; *Hellstrom et al*., 1998; *Bar-Matthews et al*., 1999; *Genty*

et al., 2003; *Drysdale et al*., 2004; *Genty et al*., 2006; *Fleitmann et al*., 2009; *Gokturk et al*., 2011; *Rudzka et al*., 2011]. However, stalagmite $\delta^{13}C$ is also affected by karst processes such as kinetic fractionation linked to the preferential degassing of $^{12}CO_2$ during $CaCO_3$ formation, whether on the stalagmite surface [*Hendy*, 1971; *Mickler et al*., 2004; *Fairchild et al*., 2006] or in conjunction with PCP [*Ihlenfeld et al*., 2003; *Johnson et al*., 2006; *Asrat et al*., 2007; *Cruz et al*., 2007; *Oster et al*., 2010]. Additional influences include, differences in bedrock $\delta^{13}C$ composition [*Fairchild et al*., 2000], seasonal changes in cave ventilation [*Spotl et al*., 2005; *Baldini et al*., 2008; *Mattey et al*., 2008; *Cosford et al*., 2009; *Frisia et al*., 2011; *Lambert and Aharon*, 2011; *Tremaine et al*., 2011], and as yet unknown biogenic processes in the soil [*Frappier et al*., 2002; *Cruz et al*., 2006]. Given the wide variety of hydrological processes, karst processes, and vegetation changes that can alter stalagmite composition, it is unclear how well trace metal ratios and $\delta^{13}C$ proxies in stalagmites reproducibly record climate changes at a given site.

[5] In this study, we use multiple cave dripwater data sets as well as three overlapping stalagmite geochemical time series to investigate the potential for Mg/Ca, Sr/Ca, and $\delta^{13}C$ as paleoclimate indicators in stalagmites from northern Borneo. We use spatial dripwater data sets collected during four separate field missions (2003, 2005, 2006, and 2008) from many caves ($N = 14$) across the same karst formation to assess the regional reproducibility of the cave dripwater trace metal ratios and $\delta^{13}C$ values. We also use a bimonthly dripwater time series to investigate whether rainfall changes correlate with cave dripwater hydrological and geochemical changes over a 2.5 year period. A high-resolution dripwater time series, comprised of hourly to daily sampling of two drips over a 3 week period, allows us to test how specific meteorological events influence dripwater geochemistry and hydrology. In the second part of the paper, we compare multiple stalagmite Mg/Ca, Sr/Ca, and $\delta^{13}C$ records that span the last 27 ka to identify potential climate-related features of the records, applying the results from the dripwater study to our analysis of the stalagmite records.

2. Study Site Geological Setting and Climate

[6] The research was conducted in caves located in Gunung Mulu (4°02′N, 114°48′E) and Gunung Buda (4°12′N, 114°56′E) National Parks, Sarawak, Malaysia (Figure 1). The caves lie within a Miocene limestone formation known as the Melinau Formation, which runs SW to NE [*Waltham and Brook*, 1980; *Wannier*, 2009]. High rainfall feeds a network of rivers that have cut steep gorges between three individual limestone mounds that are home to a large number of caves, including some of the largest and longest thus discovered [*Farrant et al*., 1995; *Despain et al*., 2003; *Farrant and Smart*, 2011]. The Gunung Mulu and Gunung Buda National Parks are tropical rainforests with thin soil cover. All dripwater samples were collected in the vadose zone, as most of the caves are ancient phreatic conduits that now lie well above the water table [*Farrant and Smart*, 2011]. The caves are characterized by large passages (up to 700 by 400 m), breakdown rooms, and streams and sumps at lower levels [*Waltham and Brook*, 1980; *Despain et al*., 2003]. The stalagmite samples were collected during a field trip to Gunung Buda National Park in October 2003 from Snail Shell Cave (4°12′20.8″N, 114°56′ 26.9″E) and Bukit Assam Cave (4°5′18 ″N, 114°57′34″E).

[7] Rainfall in northern Borneo displays prominent intraseasonal and interannual variations with a relatively small seasonal cycle. Rainfall measurements from Gunung Mulu Airport yield an average of 5 m/yr with a weak minimum during June/July [*Cobb et al*., 2007; *Partin et al*., 2007]. Interannual variations in rainfall related to the El Niño-Southern Oscillation (ENSO) are large, as evidenced by the 50% reduction in December-January-February (DJF) precipitation that occurred during the 1997/1998 El Niño event [*Cobb et al*., 2007; *Partin et al*., 2007]. Conversely, DJF rainfall increases during a La Niña event. In addition, rainfall in northern Borneo responds strongly to ocean-atmosphere interactions on intraseasonal time scales (30–90 days) [*Madden and Julian*, 1971; *Zhang*, 2005, and references therein], which accounts for ~20% of total rainfall variance at Gunung Mulu based on calculations from Mulu Airport station data [*Moerman et al*., 2013]. On-site meteorological and in-cave temperature and humidity time series collected from 2005 to 2008 reveal that above-ground temperatures range from 23 to 26°C while cave temperatures lie between 25 and 26°C with ~100% relative humidity (Onset HOBO Pro v2 data). Spot measurements of CO_2 (Telaire 7000) in various caves during the 2006 field trip were never more than 800 ppm, and in general, the caves are well ventilated because of vigorous cave circulation across large and numerous entrances.

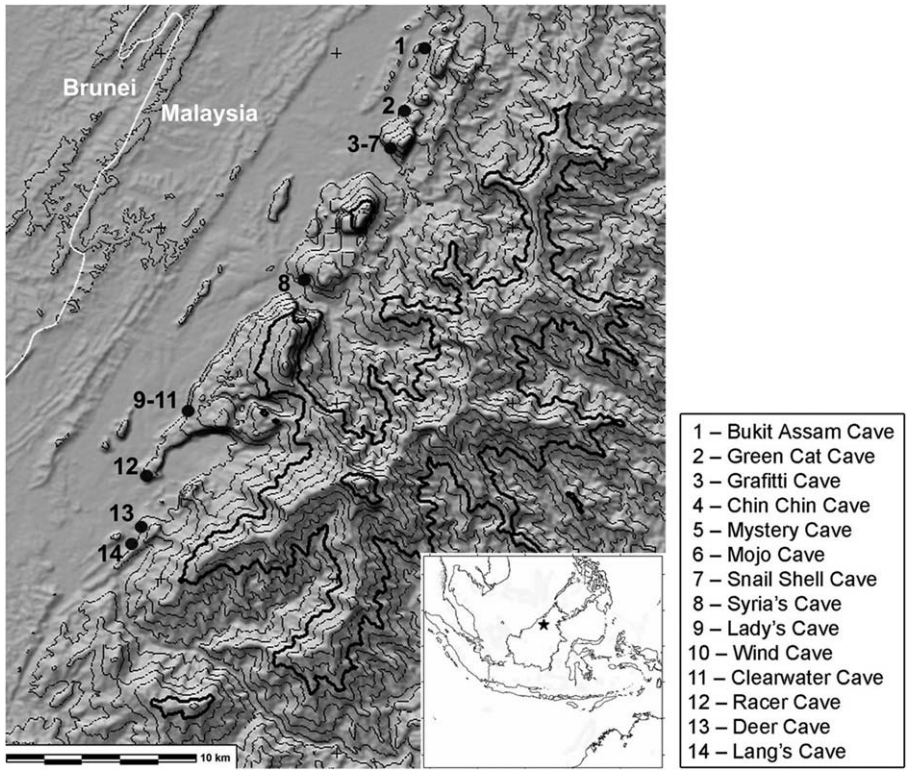

Figure 1. Topographic map of Gunung Mulu and Gunung Buda National Parks, Malaysia, showing cave locations.

3. Sampling and Analytical Methods

3.1. Overview of Data Sets

[8] Three types of data sets are presented in this paper: (1) a spatial dripwater data set from caves located throughout Gunung Mulu and Gunung Buda National Parks, (2) a temporal dripwater data set that monitors four specific drips at Gunung Mulu over ~3 years, and (3) geochemical time series from three Gunung Buda stalagmite samples spanning the last 27 kyrs. The spatial dripwater survey consists of dripwater samples collected by the authors during field missions in October 2003, March 2005, June 2006, and March 2008 from 14 caves spanning across ~30 km (Figure 1). While a few of the drips were resampled during multiple field trips, the majority are one-time samplings, with the goal of sampling as wide a range of flow regimes as possible. The temporal dripwater data set consists of dripwater samples collected by Gunung Mulu National Park officials approximately every 2 weeks from three drips spanning from 2003 to 2006: a fast-flow (WF) and slow-flow (WS) drip from Wind Cave for ~2.5 years (March 2004 to July 2006) and a slow-flow drip (L2) from Lang's Cave for ~1.5 years (March 2005 to July 2006). Drip-rate, reported in "drips per minute" (dpm) was determined by counting the number of drips that fall in 60 s. The temporal data set includes high-resolution time series collected over one and a half weeks in 2006 from drips L1 and L2 located in Lang's Cave where the drips were sampled every 3–4 h for the first 2 days and then once every 3 days for the remainder of the trip; these sites are the same locations previously reported in *Cobb et al*. [2007]. Onset HOBO Pro Series relative humidity/temperature loggers were deployed in Wind and Lang's Caves since 2005. Stalagmite samples from Snail Shell Cave (SSC01 and SCH02) formed ~250 m from the cave entrance and ~20 m from each other. The third stalagmite sample from Bukit Assam Cave (BA04), which lies ~6 km NNE from Snail Shell Cave, formed >500 m from the cave entrance. The stalagmites used in this study cover the time range from ~26 ka to present, and the oxygen isotopic ($\delta^{18}O$) time series as well as detailed chronological information for each of the three stalagmites are presented in *Partin et al*. [2007].

3.2. Bedrock and Stalagmite Geochemical Analyses

[9] Bedrock trace metal compositions were analyzed on an Agilent 7500a series Inductively Coupled Plasma Mass Spectrometer (ICP-MS) located at Georgia Tech. Bedrock samples (10–30 μg) were hand drilled with a Dremel tool fitted with a 1 mm dental bit. The powders were dissolved in 2% HNO_3 in trace-clean polypropylene tubes to yield a final Ca concentration of 3 ppm and vortexed prior to measuring. ICP-MS measurements were made using an adaptation of the procedure employed by *Schrag et al.* [1999], whereby unknown samples are bracketed by a concentration-matched gravimetrically determined synthetic standard to correct for machine drift. A 3 ppm natural standard made from a stalagmite sample was also measured at the beginning and end of each run to monitor potential matrix effects. Precisions of Mg/Ca and Sr/Ca ratios (mmol/mol) were generally ±1%, although a few measurements had errors of ±1–2%. Bedrock stable isotopic measurements were performed on a GV Isoprime-Multiprep Dual-Inlet Mass Spectrometer located at Georgia Tech (long-term 1σ reproducibility <0.05‰ for $\delta^{13}C$ and $\delta^{18}O$ based on repeat measurements of an internal standard).

[10] Stalagmite samples were cut in half, slabbed to a thickness of ~15 mm to expose the central growth axis, and polished for geochemical sampling. Mg/Ca ratios of all three stalagmites and Sr/Ca ratios of stalagmites SCH02 and BA04 were measured on a Horiba JY Ultima-C Inductively Coupled Plasma Optical Emission Spectrometer (ICP-OES) located at Georgia Tech. Trace metal ratios were measured on 30–50 μg powders drilled every 1 mm along the central growth axis (~2 mm width and ~0.5 mm depth) of the stalagmites with a 1.6 mm drill bit using a bench-top Sherline micromill model 5410. The powders were dissolved in 2% HNO_3 in an acid-cleaned polypropylene tube to yield a final Ca concentration of 30 ppm. One portion of SCH02 (the 11.8–17.4 ka time period) was run at an elevated Ca concentration of 100 ppm to bring Sr above the limit of detection on the ICP-OES. All stalagmite ICP-OES measurements were bracketed with a concentration-matched gravimetrically determined synthetic standard to correct for machine drift [*Schrag*, 1999]. Trace metal ratios of synthetic standards typically show deviations of ±0.5% (1σ, $N = 75$) over the course of a 6 h run. A stalagmite-specific known natural standard was also measured at the beginning and end of runs to monitor potential matrix effects. The $\delta^{13}C$ records from BA04 and SSC01 were measured on the GV Iso Prime Mass Spectrometer located at Georgia Tech (2σ precision of internal coral standard of ±0.17‰, $N = 245$). The $\delta^{13}C$ record from SCH02 was analyzed on a Finnigan 253 Dual-Inlet Mass Spectrometer equipped with Kiel device located at Wood's Hole Oceanographic Institute (long-term reproducibility of ±0.04‰ for $\delta^{13}C$). All $\delta^{13}C$ data are reported with respect to Vienna Pee Dee Belemnite (VPDB). Powders for stable isotopes and trace metal analyses were drilled from the same trough but at different times such that sub-millimeter offsets between these data sets may exist. Repeated tests of geochemical reproducibility demonstrated maximum offsets of <0.1 mm (<5 years given growth rates of 20 μm/yr).

3.3. Dripwater Sample Collection and Analyses

[11] Trace metal dripwater samples were collected in acid-washed, trace-clean 4 mL High-density polyethylene (HDPE) bottles. All dripwaters samples were collected by hand on-site for all drips except the slow drips of 2008. For slow drips in 2008, large-volume HDPE bottles were left out for 1–2 days to collect enough water, and then subsampled into the 4 mL HDPE bottles. Dripwaters were acidified with 10 μL of concentrated HNO_3 and centrifuged immediately prior to analysis via an Agilent (7100c) ICP-MS located at Georgia Tech. The supernatant was pipetted off and diluted tenfold with 2%HNO_3 to ~3 ppm Ca in a trace-clean polypropylene tube. Dripwater Ca concentrations were measured with precisions of ±1 ppm while dripwater Mg/Ca and Sr/Ca ratios were measured with precisions of ±3%. As with the bedrock samples, the dripwaters were bracketed by gravimetrically determined synthetic standards to correct for machine drift. A natural standard (3 ppm Ca) prepared using dissolved stalagmite powder was run at the beginning and end of the dripwater runs to monitor matrix effects.

[12] Carbon isotope dripwater samples were collected in gas-tight, crimp-top 4 mL glass vials spiked with 50 μL of $HgCl_2$ to prevent biological growth. Dripwater carbon isotope measurements were measured on a Thermo-Finnigan MAT Delta+ XP/Gas Bench located at the University of California at Santa Barbara, with a precision of ±0.1‰. Drip-rates for each drip were integrated over 60 s intervals.

Table 1. Summary of Bedrock Compositions, Where the Stable Isotope Error is 0.05‰, and the Trace Metal Ratio Error is ±1% (1σ)

Cave	$\delta^{18}O$ (‰)	$\delta^{13}C$ (‰)	Mg/Ca (mmol/mol)	Sr/Ca (mmol/mol)
Clearwater connection	−6.67	1.24	14.93	0.50
Clearwater connection	−6.62	1.03	23.65	0.32
King's Room Sample 1	−5.34	1.29	12.49	0.31
King's Room Sample 1	−6.04	0.77		
King's Room Sample 2	−4.93	1.44	15.67	0.36
King's Room Sample 2	−10.27	−1.21		
Secret Chamber	−6.09	0.61	16.45	0.68
Secret Chamber	−4.69	1.33		
Bath Hall	−4.56	1.44	16.17	0.59
Bath Hall	−4.47	1.50		
Snail Shell Sample 1	−5.60	0.82	10.37	0.35
Snail Shell Sample 1	−4.97	1.24	12.29	0.38
Snail Shell Sample 1	−5.31	0.98		
Snail Shell Sample 1	−4.96	1.21		
Snail Shell Sample 2	−5.04	1.63	8.21	0.46
Snail Shell Sample 3			2.95	0.28
Gunnung Benerat	−4.16	1.64	12.74	0.29
Gunnung Benerat	−4.24	1.69		
Lang's Cave Sample 1	−8.50	0.49	4.15	0.01
Lang's Cave Sample 1	−13.68	0.28	8.88	0.11
Lang's Cave Sample 1	−11.04	0.08		
Lang's Cave Sample 1	−11.84	−1.35		
Lang's Cave Sample 2	−6.92	1.46	35.92	0.38
Deer Cave	−8.48	1.10	45.30	0.16
Deer Cave	−8.83	1.21		
Deer Cave	−8.72	0.94		
Bukit Assam	−5.39	1.63	5.49	2.18
Bukit Assam	−4.68	1.86	5.24	2.29
Bukit Assam			5.12	1.91
Bukit Assam			8.14	1.73
Bukit Assam			8.27	2.03
Green Cat			3.28	0.47

4. Results

4.1. Bedrock Composition

[13] Bedrock samples from multiple caves contain similar Mg/Ca, Sr/Ca and $\delta^{13}C$ values whereas bedrock $\delta^{18}O$ varies appreciably (Table 1). In general, bedrock Mg/Ca ratios range from 1 to 16 mmol/mol with the exception of Lang's and Deer Cave, which contain higher values of 35–45 mmol/mol. Bedrock Sr/Ca ratios generally lie between 0.1 and 0.6 mmol/mol, although Bukit Assam Cave Sr/Ca values are higher (1.7–2.3 mmol/mol). Bedrock $\delta^{13}C$ values range between −1.5 and +1.5‰. Bedrock $\delta^{18}O$ values span a large range from −4 to −13‰, with values from Deer and Lang's Cave being consistently lighter. Different colored phases in the bedrock (white, gray, light pink and brown) do not exhibit systematic geochemical differences in either trace metal ratios or isotopic values.

4.2. Spatial Dripwater Variability

[14] Comparisons of dripwater geochemical data from three field missions allow for an assessment of the parameters that may influence dripwater geochemistry across the 30 km Melinau karst formation. This approach differs somewhat from the intensive monitoring of a single cave over time [e.g., *Fairchild et al*., 2000; *Genty et al*., 2001; *Cruz et al*., 2005; *Spotl et al*., 2005; *Treble et al*., 2005; *Banner et al*., 2007; *Fuller et al*., 2008; *Lorrey et al*., 2008; *Bradley et al*., 2010; *Jex et al*., 2010; *Boch et al*., 2011; *Frisia et al*., 2011; *Schimpf et al*., 2011; *Lambert and Aharon*, 2011; *Tremaine et al*., 2011; *Partin et al*., 2012], yet is complementary in that one can search for geochemical relationships predicted via PCP across ∼150 different drip sites over several years. The sampling of a large number of drips attempts to cover the range of flow regimes in the karst. Cross-plots of Metal/Ca ratios versus dripwater [Ca] are used to assess the influence of PCP on dripwater geochemistry [*Fairchild et al*., 2000]. Appreciable scatter in the data from northern Borneo suggests no clear PCP control on dripwater trace metal chemistry (Figures 2a and 2b). However, dripwater Mg/Ca and Sr/Ca values are generally higher than corresponding bedrock values (Figures 2a and 2b), consistent with a role for PCP.

[15] No clear relationship exists between drip-rate and dripwater geochemistry, although slower drips tend to have the highest Mg/Ca and Sr/Ca values (Figure 3). Low Mg/Ca and Sr/Ca values were measured in drips exhibiting a wide range of drip-rates, implying that drip-rate alone has no discernable effect on dripwater trace metal ratios at our site.

[16] We uncover a clear relationship between dripwater $\delta^{18}O$ and Mg[Sr]/Ca, whereby high-Mg[Sr]/Ca drips have relatively similar $\delta^{18}O$ values, while low-Mg/Ca drips exhibit a broad range of $\delta^{18}O$ values (Figure 4). For those drips with high Mg/Ca (or Sr/Ca), dripwater $\delta^{18}O$ converges to the annual mean dripwater $\delta^{18}O$ value of −6.7‰ per mil reported in *Cobb et al*. [2007]. This "pyramid" structure of dripwater $\delta^{18}O$ versus Mg/Ca (or Sr/Ca) is observed in both the spatial and temporal dripwater data sets (Figures 4a and 4b, respectively).

4.3. Temporal Dripwater Variability

[17] The three temporal dripwater data sets display prominent subseasonal variations in dripwater

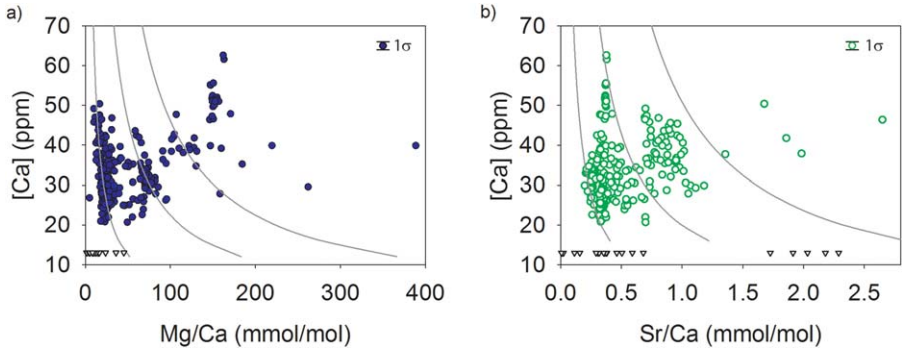

Figure 2. Dripwater geochemistry of the spatial dripwater data set for the caves in Figure 1. (a) [Ca] versus Mg/Ca, (b) [Ca] versus Sr/Ca. Curved gray lines in each figure represent geochemical trajectories for waters that experience PCP in the epikarst [*Fairchild et al*., 2000], using values of $D_{Mg} = 0.04$ and $D_{Sr} = 0.1$ [*Huang and Fairchild*, 2001]. Upside-down triangles represent the bedrock compositions listed in Table 1. The error (1σ) for [Ca] is depicted graphically while the error bars (1σ) for Mg/Ca and Sr/Ca are smaller than the size of the symbol.

geochemistry, with no coherent annual to interannual variations over the 2.5 year interval (Figure 5). All three drips have similar [Ca] while both Wind Cave drips, WS and WF, have consistently higher $\delta^{13}C$, higher Sr/Ca and lower Mg/Ca than the Lang's Cave drip, L2. The disparity between the dripwater time series (Figure 5 and Table 2) implies that dripwater geochemical variability is likely governed by processes that are unique to a drip's hydrological pathway through the karst system at the site. However, rainfall amount can influence dripwater $\delta^{13}C$, and, to a lesser extent, dripwater Sr/Ca at the site over a period of several months (Table 3). For example, Drip WS has a ln(Mg/Ca) versus ln(Sr/Ca) slope of 0.71, closest to the theoretical slope of 0.88 [*Sinclair*, 2011] suggesting that PCP exerts a strong control on trace metal ratios at this site—a conclusion that is not evident when viewing the individual time series. Drip L2 has a ln(Mg/Ca) versus ln(Sr/Ca) slope of 0.31 and WF has a slope of −0.04 confirming the visual evidence of a reduced influence

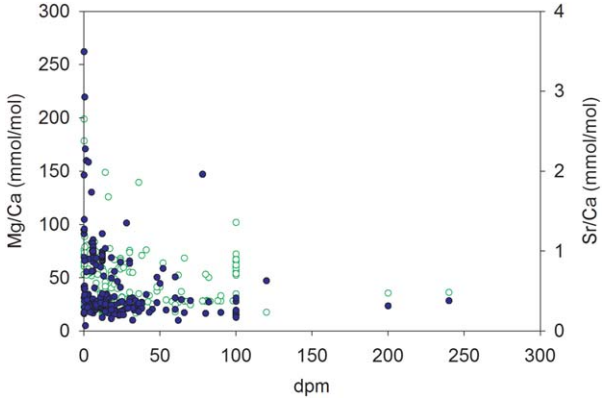

Figure 3. Cross-plot of Mg/Ca (blue closed circles) and Sr/Ca (green open circles) versus drips per minute (dpm) for entire dripwater data set.

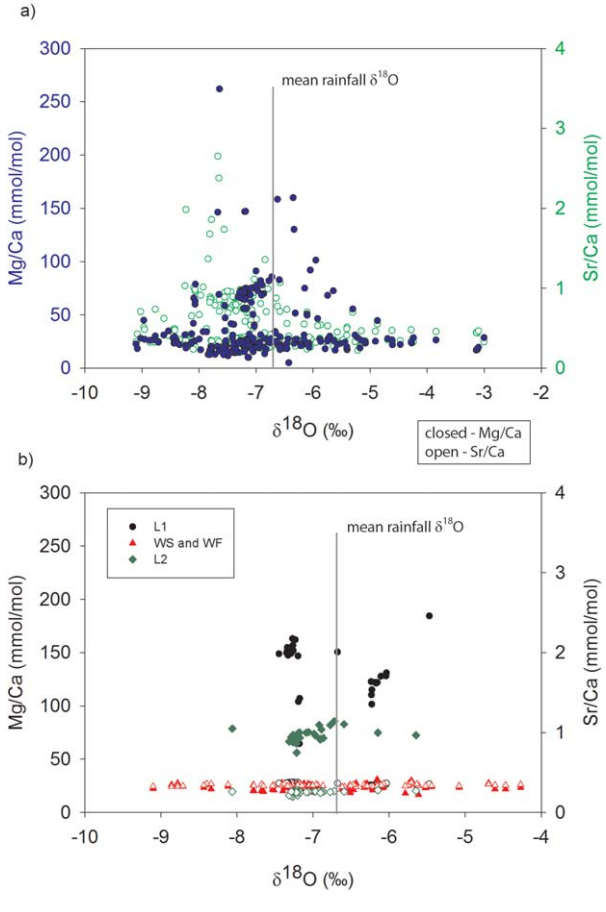

Figure 4. Cross-plot of (Mg/Ca (blue closed circles) and Sr/Ca) (green open circles) versus $\delta^{18}O$ for (a) all dripwaters and (b) the temporal data sets (closed points - Mg/Ca and open points - Sr/Ca). The vertical line represents mean rainfall $\delta^{18}O$.

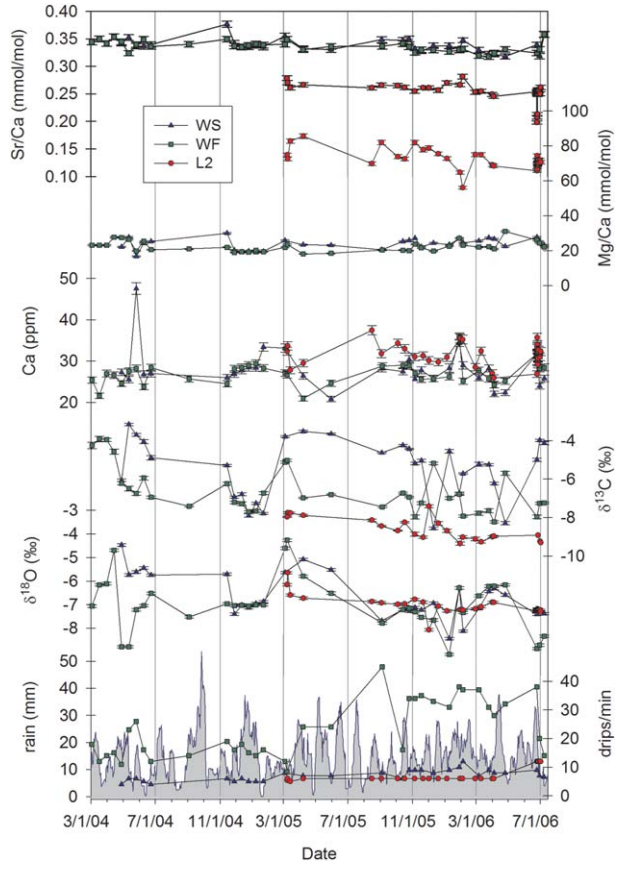

Figure 5. Time series of dripwater geochemistries for drips WS (blue triangles), WF (green squares), and L2 (red circles). Plotted are Sr/Ca, Mg/Ca, [Ca], $\delta^{13}C$, $\delta^{18}O$, drip-rate, and a 9 day running mean of rainfall from nearby Mulu airport (provided by the Sarawak Department of Irrigation and Drainage, Malaysia). The error (1σ) for [Ca] is depicted graphically while the error bars (1σ) for Mg/Ca, Sr/Ca, $\delta^{13}C$, and $\delta^{18}O$ are smaller than the size of the symbol.

by PCP on trace metal ratios, much like the result for section 4.2 of the entire dripwater data set (Figures 2a and 2b), most likely due to short residence times that do not allow appreciable PCP-driven enrichments in Mg(Sr)/Ca ratios to occur.

[18] Two drips in Lang's Cave collected at 2–3 h intervals for 2 days and then once a day for a period of 1 week during the 2006 field trip provide a test of how specific meteorological events influence dripwater geochemistry and hydrology at Mulu (Figure 6). Preceding our arrival on 23 June 2006, rainfall at Gunung Mulu averaged ~30–50 mm/d over a period of ~7 days. By June 26, rainfall effectively ceased (<1 mm/d) for approximately 2 weeks. The relatively slow-dripping drip L2 (~12 dpm) showed little change in drip-rate over the entire 3 week field trip, (Figure 4) while the relatively fast-dripping drip L1 (~100 dpm) began to decrease 1 day after the rainfall stopped and was dripping at 5 dpm by the end of the sampling period 1 week later (Figure 4). Over that week, drip L1 Mg/Ca ratios decreased by 35%, and its [Ca] decreased by 30%, opposite to the response expected from PCP (wherein reduced rainfall should allow more time for PCP to occur and thereby increase drip Mg/Ca ratios). We hypothesize that the observed decreases in L1's

Table 2. Correlation of Time Series Dripwater Data from Drips in Wind Cave and Lang's Cave

Chemical Variables	R
	Wind Cave Fast Drip (WF)
$\delta^{18}O$ vs. $\delta^{13}C$	0.44**
$\delta^{13}C$ vs. Sr/Ca	0.52**
	Wind Cave Slow Drip (WS)
$\delta^{13}C$ vs. Mg/Ca	0.34*
[Ca] vs. Mg/Ca	−0.34*
$\delta^{13}C$ vs. Sr/Ca	0.35*
	Lang's Cave Slow Drip (L2)
[Ca] vs. Mg/Ca	−0.40*

**99% significant.
*95% significant.
Calculated with Student's t-test.

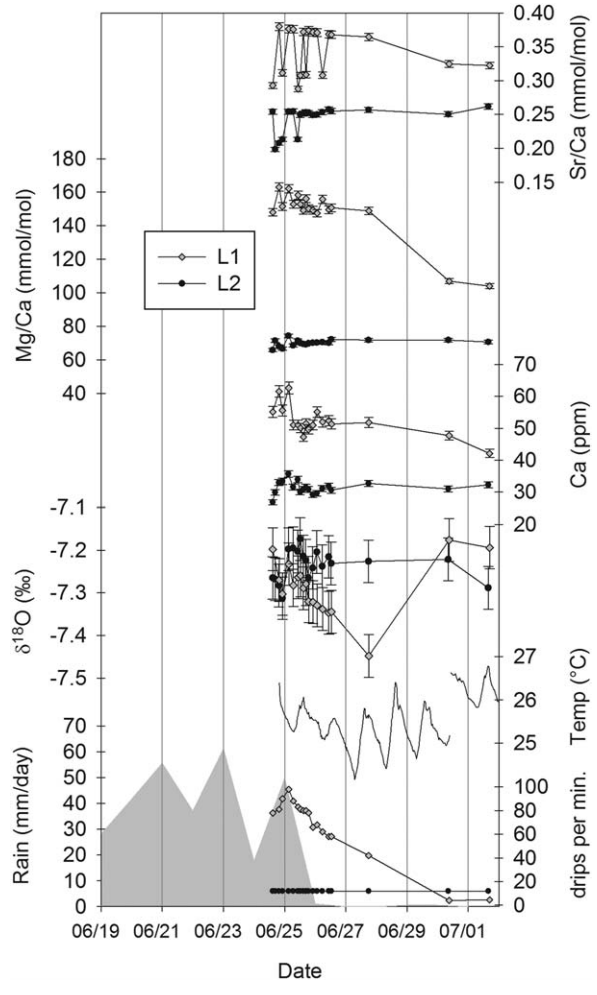

Figure 6. High-resolution hourly dripwater time series for L1 (empty diamonds) and L2 (filled circles) from Lang's Cave.

Mg/Ca and [Ca] values may reflect the arrival of older karst water whose geochemistry was set during the preceding wet period given dripwater residence times of ~2–3 months previously documented in another area of the same cave system [*Cobb et al*., 2007].

[19] The temporal drips show the same behavior as the spatial dripwater data set in $\delta^{18}O$ versus Mg/Ca (or Sr/Ca) space with little dependence on drip-rate (Figure 4b). The drips from Wind Cave (WS and WF) span the majority of the range of dripwater $\delta^{18}O$ values (i.e., −4.2 to −9‰), with low Mg(Sr)/Ca, and possess markedly different drip-rates. These drips would both be categorized as seepage flow based on their relatively constant drip-rates. The drips from Lang's Cave (L1 and L2) have less $\delta^{18}O$ variability and higher Mg(Sr)/Ca, where L2's drip-rate is slow and invariable and L1's drip-rate is fast and highly variable (L1). Drip L2 may be categorized as a diffuse flow drip, while drip L1 is mainly activated during rain events based on its discharge variability. It is worth noting that despite the heterogeneity of flow conditions implied by the temporal drips, they display $\delta^{18}O$ versus Mg/Ca (or Sr/Ca) relationships that are similar to the spatial dripwater $\delta^{18}O$-Metal/Ca relationships (Figures 4a and 4b). Again, we conclude that drip-rate is not a good diagnostic indicator of geochemical processes occurring upstream of a given drip site in northern Borneo, contrary to what has been observed at some midlatitude sites [*Tooth and Fairchild*, 2003; *Fairchild et al*., 2006b].

4.4. Stalagmite Geochemical Data

[20] Stalagmite Mg/Ca ratios, Sr/Ca ratios, and $\delta^{13}C$ records from SSC01, SCH02, and BA04 are characterized by different absolute values and patterns of variability over the last 27 kyrs. Samples SSC01 (Figure 7), SCH02 (Figure 8), and BA04 (Figure 9) have different means and different magnitudes of variability in Mg/Ca and Sr/Ca, and the magnitude of the centennial-scale Mg/Ca and Sr/Ca variability is proportional to the absolute value of Mg/Ca and Sr/Ca (i.e., higher magnitude centennial-scale variability is associated with higher absolute Mg/Ca values) (Figures 7–9). The stalagmite Mg/Ca and Sr/Ca records are all characterized by substantial centennial-scale variability superimposed on different glacial-to-

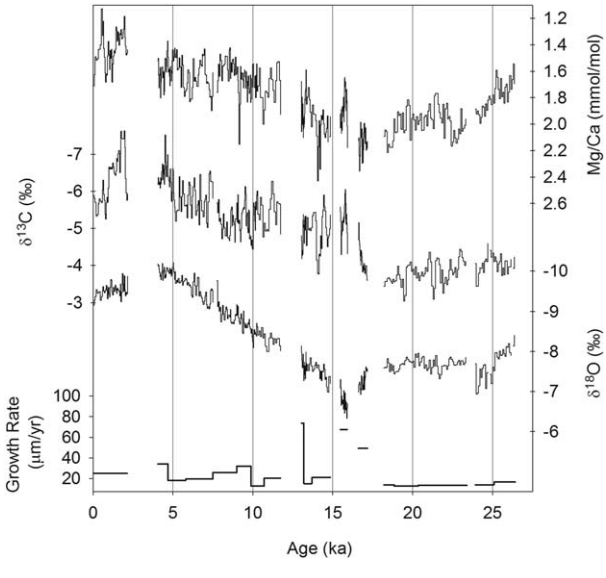

Figure 7. Geochemical time series of stalagmite SSC01 over the last 27ka. Plotted are Mg/Ca ratio, $\delta^{13}C$, $\delta^{18}O$, and growth rate. Age models for the samples are discussed in *Partin et al*. [2007].

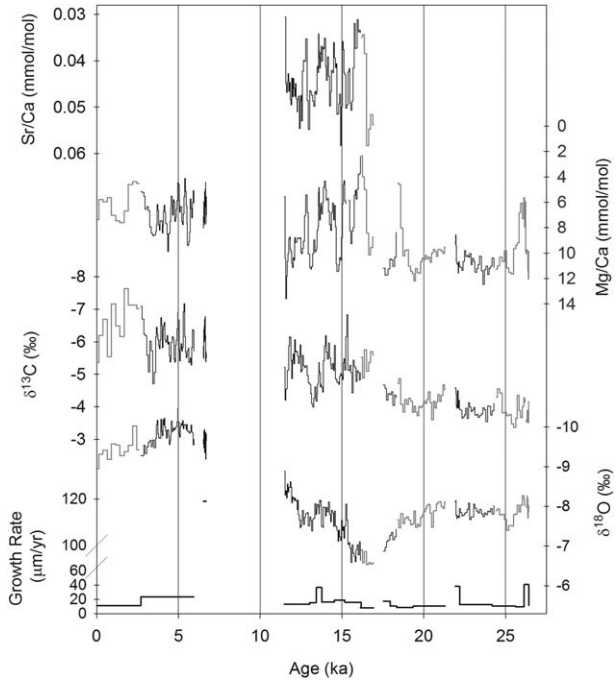

Figure 8. Same as Figure 5 but for stalagmite SCH02. Also included are Sr/Ca ratios (via ICP-OES). Data with growth rates less than 10 μm/yr are colored in gray, and are considered untrustworthy for paleoclimatic interpretation due to uncertainty in age models associated with the presence of unresolved hiatuses.

interglacial trends. The sign of the glacial-to-interglacial Mg/Ca trends in SCH02 and SSC01 exhibit a linear decrease whereas Mg/Ca and Sr/Ca in BA04 exhibit linear increases. All three stalagmite $\delta^{13}C$ records are characterized by centennial-scale variability of ~1.5–2‰ superimposed on a glacial-to-interglacial decrease of ~2‰ (Figure 10), where SCH02 and SSC01 approximately overlap in mean value but BA04 is 4‰ more enriched. None of the Mg/Ca, Sr/Ca, or $\delta^{13}C$ stalagmite records replicate as well as the $\delta^{18}O$ stalagmite records [*Partin et al.*, 2007].

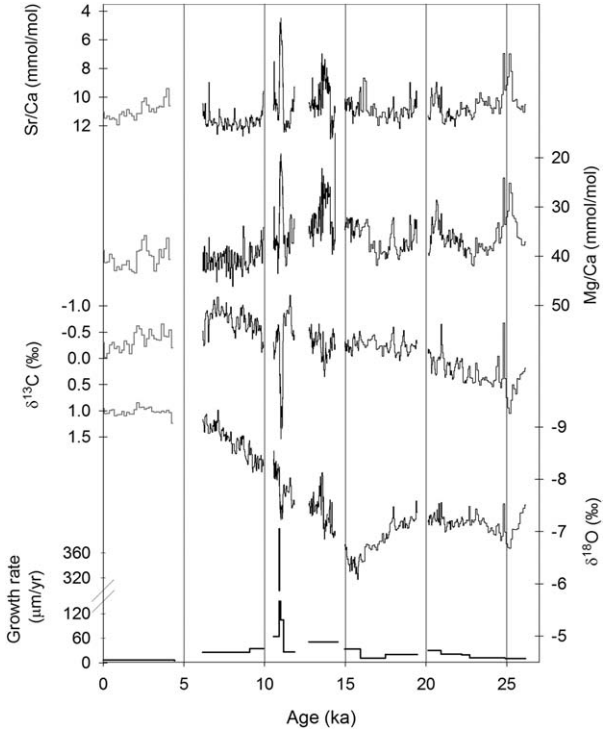

Figure 9. Same as Figure 6 but for stalagmite BA04.

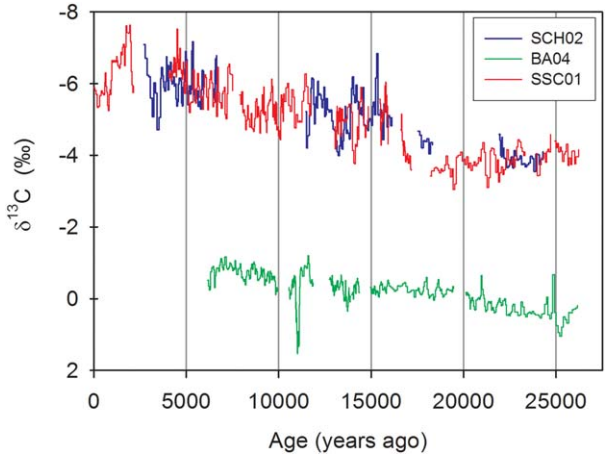

Figure 10. Stalagmite $\delta^{13}C$ for all three stalagmites.

Table 3. Correlation of Time Series Dripwater Data with Mulu Airport Rainfall Measurements

	R	R	R
Chemical Variable vs. Rain	Drip WF	Drip WS	Drip L2
δ^{18}O vs. 1-month rain mean	ns	ns	−0.47*
δ^{18}O vs. 3-month rain mean	ns	ns	−0.47*
δ^{18}O vs. 6-month rain mean	ns	−0.44*	ns
δ^{13}C vs. 1-month rain mean	−0.33*	−0.39*	ns
δ^{13}C vs. 3-month rain mean	−0.50**	−0.44*	−0.57*
δ^{13}C vs. 6-month rain mean	−0.47**	−0.40*	−0.50*
Mg/Ca vs. 1-month rain mean	ns	ns	ns
Mg/Ca vs. 3-month rain mean	ns	ns	ns
Mg/Ca vs. 6-month rain mean	ns	ns	ns
Sr/Ca vs. 1-month rain mean	−0.34*	ns	ns
Sr/Ca vs. 3-month rain mean	−0.54**	−0.36*	ns
Sr/Ca vs. 6-month rain mean	−0.54**	−0.43*	ns

**= 99% significant.
*= 95% significant.
ns = not significant (<95%).
Calculated with Student's t-test.

[21] The Mg/Ca, Sr/Ca, or δ^{13}C records within one stalagmite do not reproduce consistent changes expected from a karst process such as PCP. PCP predicts significant correlations between stalagmite Mg/Ca, Sr/Ca, or δ^{13}C [*Fairchild et al.*, 2000; *Johnson et al.*, 2006]. Mg/Ca and Sr/Ca ratios in SCH02 (Table 4) and BA04 (Table 5) are positively correlated; sample BA04 has a ln(Mg/Ca) versus ln(Sr/Ca) slope of 0.99, and the slope for SCH02 is 0.3. Also, Mg/Ca, and δ^{13}C in SCH02 and SSC01 (Tables 4 and 6) are positively correlated. However in BA04, the sample thought to have the most PCP at the drip site (having the highest Mg/Ca and Sr/Ca values and also the closest slope [0.99] to the theoretical slope [0.88]), Mg/Ca (and Sr/Ca), and δ^{13}C in BA04 are negatively correlated.

[22] Similarly, the Mg/Ca, Sr/Ca, and δ^{13}C proxy records do not show consistent changes between the stalagmites, except for the glacial-interglacial trend in δ^{13}C. To calculate correlations between stalagmite records of varying temporal resolutions, the raw records are first smoothed using a 200 year running mean and then sampled at regular 200 year intervals. Analyzing the entire 27 kyr interval as a whole, stalagmite δ^{13}C and trace metal records correlations are low ($R = 0.02$–0.15) and not significant. However, portions of the trace metal ratios and δ^{13}C records show significant, positive covariations between samples (e.g., for δ^{13}C, $R = 0.76$, $p < 0.01$ between SCH02 and SSC01 from 0 to 2200 ka), suggesting that PCP may play a role in driving some portion of the geochemical variability during some time intervals, probably in response to hydrological forcing (Table 6). To address the

Table 4. Intra-stalagmite Geochemical Comparisons: SCH02

Time Period (ka)	δ^{18}O-δ^{13}C	δ^{18}O-Mg/Ca	δ^{13}C-Mg/Ca	δ^{18}O-Sr/Ca[a]	δ^{13}C-Sr/Ca[a]	Mg/Ca-Sr/Ca[a]
0-6103	−0.01	0.04	**0.44****			
6689-6888	0.18	−0.05	0.34			
11741-17433	0.11	**−0.31****	**0.26***	−0.02	−0.07	**0.74****
18225-21956	−0.12	0.19	**0.47****			
22583-27226	**0.26***	**0.51****	0.21			
Overall R (Weighted Avg)	**0.09**	**0.04**	**0.33**			

[a]Denotes that the sample was run at 100ppm [Ca].
**99% significant.
*95% significant.
Calculated with Student's t-test.

Table 5. Intra-stalagmite Geochemical Comparisons: BA04

Time Period (ka)	δ^{18}O-δ^{13}C	δ^{18}O-Mg/Ca	δ^{13}C-Mg/Ca	δ^{18}O-Sr/Ca	δ^{13}C-Sr/Ca	Mg/Ca-Sr/Ca
6327-10229	**0.61****	**−0.26****	−0.12	**−0.21***	**−0.49****	**0.32****
10854-12188	**0.65****	**−0.75****	**−0.64****	**−0.85****	**−0.90****	**0.93****
13105-14777	0.14	−0.04	0.21	**−0.46****	**−0.63****	**0.61****
15338-20036	−0.06	**−0.51****	**−0.23***	**0.22***	0.15	**0.66****
20721-27010	**0.71****	−0.08	−0.12	0.04	−0.19	**0.77****
Overall R (Weighted Avg)	**0.43**	**−0.32**	**−0.17**	**−0.23**	**−0.39**	**0.65**

**99% significant.
*95% significant.
Calculated with Student's t-test.

Table 6. Intra-stalagmite Geochemical Comparisons: SSC01

Time Period (ka)	δ^{18}O-δ^{13}C	δ^{18}O-Mg/Ca	δ^{13}C-Mg/Ca
0-2203	**0.31***	0.25	**0.52****
4145-11823	**0.66****	**0.30****	**0.16***
13396-15272	0.02	0.27	**0.30***
15906-17667	**−0.65****	**−0.60****	**0.76****
18725-24078	0.17	−0.04	0.26
24623-27228	0.20	**0.64****	**0.24****
Overall R (Weighted Avg)	**0.24**	**0.14**	**0.32**

**99% significant.
*95% significant.
Calculated with Student's t-test.

possibility that the age models for the stalagmite records do not accurately constrain the prominent centennial-scale variability, we attempted to wiggle-match portions of the Mg/Ca and δ^{13}C records within the limit of dating uncertainties (±400 years for ages younger than 11 ka or ±2% for ages older than 11 ka). The wiggle-matched chronologies marginally improved the correlations between the records in four out of seven attempts. Adjusting the records within the errors in the age model can account for a portion of the mismatches between stalagmites but cannot fully explain the low correlations.

[23] Paleo-dripwater geochemistry for each stalagmite is estimated by dividing measured stalagmite Mg/Ca and Sr/Ca ratios by average distribution coefficients for Mg^{2+} and Sr^{2+} in calcite [*Huang and Fairchild*, 2001]. Samples SSC01 (30–60 mmol/mol for Mg/Ca, 0.5 mmol/mol for Sr/Ca) and SCH02 (60–285 mmol/mol for Mg/Ca, 0.3–0.5 mmol/mol for Sr/Ca) have estimated dripwater concentrations in the range found in the modern survey. However, sample BA04 has 520–1125 mmol/mol for Mg/Ca and 45–129 mmol/mol for Sr/Ca, much higher than dripwater values sampled to date. Comparing the paleo-dripwaters to the modern dripwaters would indicate that PCP has less influence on SSC01 and more on BA04, with SCH02 being in the middle.

5. Discussion

5.1. Controls on Dripwater and Stalagmite Geochemistry

5.1.1. Bedrock Influences

[24] Some studies suggest that overlying bedrock composition [*Fairchild et al*., 2000] and dripwater drip-rate [*Fairchild et al*., 2000; *McDonald et al*., 2004; *Musgrove and Banner*, 2004; *Baldini et al*., 2006; *Cruz et al*., 2007] affect dripwater geochemistry, yet these factors only partially explain observed changes in dripwater geochemistry in northern Borneo. For one, bedrock composition across the formation is mostly low-Mg calcite, limiting the potential impact of incongruent dolomite dissolution and of dissolution rate differences between calcite and dolomite. Higher dripwater Mg/Ca ratios in Lang's cave at site L1 (40–160 mmol/mol) (Figure 2a) may be influenced by bedrock values of 36 mmol/mol (Table 1). Bukit Assam Cave bedrock, located in the Buda region, contains ∼2 mmol/mol Sr/Ca (Table 1 and triangles in Figure 2b) and dripwater Sr/Ca in Bukit Assam Cave consistently have the highest values (∼2 mmol/mol) (Figure 2b). The higher bedrock Sr/Ca values may explain a portion of the higher dripwater Sr/Ca values without invoking a geochemical mechanism such as PCP. We find no connection between bedrock δ^{13}C and dripwater or stalagmite δ^{13}C [*Genty et al*., 2001]. Notably, bedrock δ^{18}O values span ∼9‰, but the dripwater and stalagmite δ^{18}O data are highly reproducible supporting the use of stalagmite δ^{18}O as a record of rainfall δ^{18}O with little overprint from karst processes.

5.1.2. Residence Time

[25] We find that in northern Borneo changes in rainfall δ^{18}O and mixing (the latter enhanced by increased dripwater residence times) control dripwater δ^{18}O, while at some sites Mg/Ca and Sr/Ca are influenced by the extent of PCP (function of residence time) and bedrock to a minor extent. Despite the lack of a strong correlation between drip-rate and Mg/Ca (Sr/Ca) ratios, slow drips on average have higher trace metal ratios (Figure 3) and δ^{18}O values close to the mean annual rainfall δ^{18}O value at our site (Figures 4a and 4b). Assuming that some of the slow drips have long residence times, then the higher Mg/Ca and Sr/Ca ratios result from slow, diffuse flow that have increased reaction time in the epikarst and vadose zone [*Fairchild et al*., 2000; *McDonald et al*., 2004; *Musgrove and Banner*, 2004; *Baldini et al*., 2006; *Cruz et al*., 2007]. The similarity between the pattern of geochemical variability in the temporal and spatial drips (Figures 4a and 4b) suggests that the spatial study of drips likely samples the range of flow regimes (i.e., residence times) in northern Borneo, as the temporal drips have a range of discharge characteristics.

[26] It is important to note that the temporal data do not support a direct correlation between drip-rate and flow type, as observed at predominantly midlatitude sites, whereby slow drips are

associated with diffuse/seepage flow and fast drips represent fracture flow [*Fairchild et al.*, 2006b]. For example, drips L2 and WS are both seepage flow based on discharge. However, the two slow drips display very different $\delta^{18}O$ and Mg(Sr)/Ca values such that only L2 would be considered a diffuse flow geochemically (close to mean $\delta^{18}O$ and high Mg(Sr)/Ca) and WS would be considered fracture flow (variable $\delta^{18}O$ and low Mg(Sr)/Ca). Drips WF and L1 are both fast drips, however drip L1 behaves more like a diffuse flow geochemically (close to mean $\delta^{18}O$ and high Mg(Sr)/Ca) despite the fact that the drip-rate went from 100 to 5 dpm in 2 weeks time, which would suggest a fracture flow drip based on discharge. Our data suggest that in northern Borneo we cannot rely on the traditional hydrologic indicator of drip-rate to classify a drip's hydrological state, but instead must use its geochemical characteristics to infer its flow regime.

[27] Two lines of evidence point toward the importance of residence time as a primary control on the geochemistry of dripwaters at Gunung Mulu:

[28] 1. In most, though not all, cases, dripwater Mg[Sr]/Ca ratios tend to increase as drip-rate decreases, supporting the notion that PCP is enhanced as residence time increases.

[29] 2. Elevated dripwater Mg/Ca values are associated with a narrow range of dripwater $\delta^{18}O$ values scattered about the mean annual rainfall $\delta^{18}O$ value, suggesting that PCP preferentially occurs along pathways characterized by long residence times that also allow for appreciable mixing.

[30] The observed responses of drip-rates and drip geochemistry to large rainfall variations through time can be explained using a simple model for how rainfall changes translate into hydrological and geochemical variations at a drip site (Figure 11). In our model, drip-rate responds instantaneously to rainfall changes via changes in hydraulic loading that are felt throughout the karst system. Dripwater Mg/Ca, Sr/Ca and $\delta^{13}C$ responses lag the drip-rate response, as processes such as calcite precipitation, dissolution, and CO_2 degassing processes act on water that is located throughout the epikarst and vadose zones. Rainfall changes impact overall aridity in the karst environment cumulatively through time, such that PCP accumulates during successive dry times, driving increases in dripwater Mg[Sr]/Ca and $\delta^{13}C$ values. Dripwater $\delta^{18}O$ is the last to respond in this model, as changes in dripwater $\delta^{18}O$ only occur after the rainwater itself has transited the entire flow path-

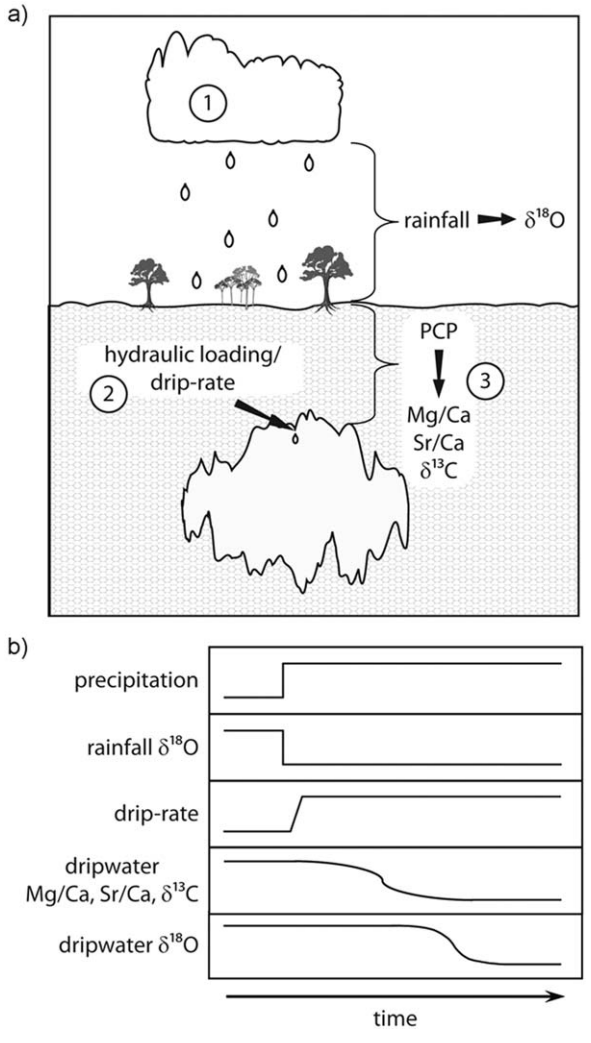

Figure 11. Schematic of a potential sequence of processes that affect dripwater flow rate and geochemistry. First, rainfall $\delta^{18}O$ changes at the rainwater infiltration sites when precipitation falls. Next, drip rates respond to changes in hydraulic pressure. Then, dripwater Mg/Ca, Sr/Ca, and $\delta^{13}C$ change in response to PCP in the epikarst and vadose zone. Lastly, dripwater $\delta^{18}O$ changes after surface waters have reached the drip site.

way. This sequence of events, combined with the complexity of flow paths in the Borneo karst system (whereby "slow" and "fast" drips can have similar geochemical characteristics), explains why the effects of PCP can be decoupled from both drip-rate and drip $\delta^{18}O$ in the observed dripwater data sets form Borneo.

[31] Limited evidence of PCP in the full northern Borneo dripwater data set may be due in part to higher annual rainfall (~5 m/yr) and reduced seasonality of rainfall that leads to the rapid transport of water through the epikarst and vadose zone year round. For the relatively fast drips sampled in this study, large rainfall amounts likely lead to

relatively low residence times, making the system more susceptible to individual meteorological events. On the other hand, slow drips, whose upstream water resides long enough in the epikarst for PCP to occur, are more likely to record climate conditions in their geochemistry [*Baldini et al*., 2006]. Second, the lack of a pronounced dry season in northern Borneo might keep Mg/Ca values relatively low (30–50 mmol/mol), and therefore more difficult to distinguish against a backdrop of highly variable Mg/Ca in our caves which is set initially by other conditions, e.g., bedrock dissolution or soil leaching. By contrast, drier, midlatitude sites are characterized by much higher absolute values and ranges in dripwater Mg/Ca ratios, 50–500 mmol/mol, and Sr/Ca, 1–13 mmol/mol, [*Fairchild et al*., 2006a; *Cruz et al*., 2007]—evidence that PCP is probably more effective in these settings with increased seasonality. The importance of rainfall seasonality in enhancing PCP is highlighted in a cave study from Guam, where a long dry season allows time for appreciable PCP to occur leading to high Mg/Ca (350–600 mmol/mol) and low Ca (40 mmol/mol) values in the dry season [*Partin et al*., 2012].

[32] The dripwater Ca concentrations in Gunung Mulu (20–65 ppm) are lower than in the midlatitudes (80–500 ppm) [e.g., *Fairchild et al*., 2000; *Genty et al*., 2001; *Cruz et al*., 2005; *Spotl et al*., 2005; *Treble et al*., 2005; *Banner et al*., 2007; *Fuller et al*., 2008; *Lorrey et al*., 2008; *Bradley et al*., 2010; *Jex et al*., 2010; *Boch et al*., 2011; *Frisia et al*., 2011; *Schimpf et al*., 2011], despite the high productivity (and presumably high soil pCO_2) of a rain forest above the caves. The low [Ca] values in Borneo are likely indicative of a short residence time that does not allow for supersaturation of karst waters with respect to calcite to occur. The study from the tropical site in Guam also supports this hypothesis—the dry season [Ca] values in Guam, which are reduced relative to wet season due to PCP, are approximately equal to the highest Ca values in Borneo [*Partin et al*., 2012]. Interestingly, mean U concentrations in the stalagmites are highly correlated to mean stalagmite Mg/Ca and Sr/Ca ratios (BA04 > SCH02 > SSC01) [*Partin et al*., 2007], suggesting that many metals may be enriched in the karst waters via PCP, to varying degrees. This observation agrees with similar results based on stalagmites from Israel [*Ayalon et al*., 1999] and Australia [*Treble et al*., 2003; *Treble et al*., 2005], but is opposite to geochemical patterns observed in a Chinese stalagmite [*Johnson et al*., 2006].

Table 7. Inter-stalagmite Geochemical Comparisons

BA04 & SCH02 Time Period (ka)	δ18O	δ13C	Mg/Ca	Sr/Ca
13186-14697	0.04	-0.23	0.59	0.65
15468-17369	−0.31	-0.11	**0.71***	0.51
18283-19961	0.39	0.18	−0.63	
20807-21906	0.01	0.05	0.31	
22663-26960	**0.70****	**0.43***	−0.07	
Overall R	**0.29**	**0.15**	**0.12**	**0.58**
BA04 & SSC01 Time Period (ka)	**δ18O**	**δ13C**	**Mg/Ca**	
6409-7635	0.28	−0.21	−0.12	
8009-10139	**0.72***	−0.11	**−0.60***	
10950-11748	−0.11	−0.09	0.42	
13488-14697	0.71	−0.32	0.03	
15998-17575	**0.84****	0.01	0.31	
18798-19961	0.22	−0.02	0.73	
20807-24001	0.43	−0.31	0.41	
24698-26960	0.38	0.05	**0.58***	
Overall R	**0.47**	**−0.14**	**0.22**	
SCH02 & SSC01 Time Period (ka)	**δ18O**	**δ13C**	**Mg/Ca**	
67-2122	**0.73***	**0.76**	0.12	
4236-6037	0.36	−0.10	0.47	
13488-15120	0.65	−0.23	−0.41	
15998-17369	**-0.80***	−0.56	−0.20	
18798-21906	0.08	0.15	−0.74**	
22663-24001	-0.15	−0.61	−0.48	
24698-27153	0.16	−0.02	0.36	
Overall R	**0.18**	**−0.02**	**−0.13**	

**99% significant.
*95% significant.
Grey number <95%.
Calculated with Student's t-test.

5.2. Stalagmite Mg/Ca, Sr/Ca, and δ^{13}C Records as Records of Paleo-Rainfall

[33] Short time periods of covariation in the stalagmite records of Mg/Ca, Sr/Ca, and δ^{13}C (Table 7) are best explained by rainfall variability, which modulates PCP in the karst. Generally, the covarying portions of the stalagmite geochemical time series exhibit prominent centennial-scale variability, perhaps indicating either (1) a preferred time scale for the PCP mechanism at our site and/or (2) appreciable rainfall variability on centennial timescales.

[34] Two distinct types of rainfall changes could affect the degree of PCP in the northern Borneo caves. For one, an average reduction in rainfall may occur without a change in the seasonality of rainfall, leading to an increase in evaporative effects/CO_2 degassing and increased PCP. Alternatively, a change in the distribution of rainfall may occur such that there are longer break periods between rainfall events (increased seasonality),

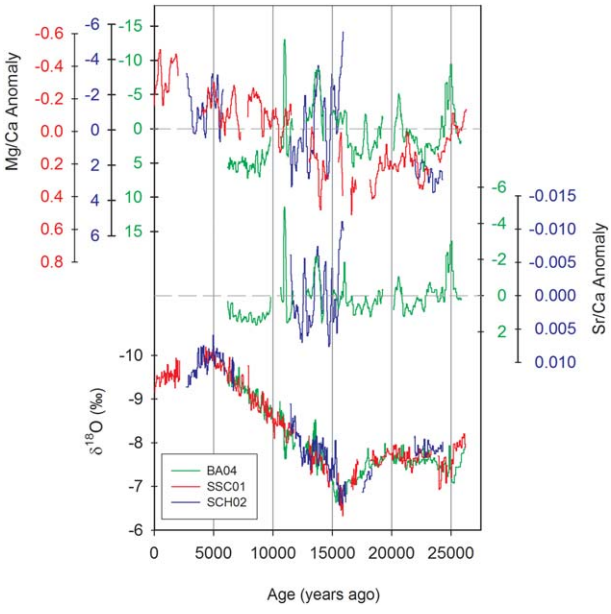

Figure 12. Stalagmite Mg/Ca anomalies, Sr/Ca anomalies, and $\delta^{18}O$ for all three stalagmites. The trace metal data have been smoothed by a 200 year moving average discussed in the text (see section 4.4.2). Data with growth rates less than 10 μm/yr are not included (see Figure 6).

with or without a change in total annual rainfall. Groundwater is not recharged during dry periods, so evaporative effects and degassing of CO_2 lead to PCP that will increase trace metal ratios in dripwaters. Indeed, seasonal changes in trace metal ratios observed in high-resolution studies of stalagmites from China [*Johnson et al*., 2006], Australia [*Treble et al*., 2003, 2005], and Guam [*Partin et al*., 2012] are directly linked to alternating wet and dry seasons. However, because the stalagmite measurements represent 50–100 year averages, it is not possible to distinguish between a reduction in average annual rainfall versus a change in seasonality. Future high-resolution records from fast-growing stalagmites in the area may enable one to distinguish between seasonal versus subseasonal controls on stalagmite geochemical variability.

5.3. Potential Climate Changes Over the Last 30 ka in Northern Borneo

[35] Several new pieces of information are revealed about climate in northern Borneo over the last 27 ka by focusing on shared features in the Mg/Ca, Sr/Ca, and $\delta^{13}C$ of the three stalagmite records. During the Last Glacial Maximum (LGM), defined here as the time period from 19 to 23 ka, stalagmite Mg/Ca ratios are higher in SCH02 and SSC01 (Figure 12). Higher stalagmite Mg/Ca ratios suggest that rainfall was reduced during the LGM. Stalagmite Mg/Ca and $\delta^{13}C$ evidence for reduced LGM precipitation is important, given the somewhat ambiguous interpretation of increased stalagmite $\delta^{18}O$ values during the LGM (Figure 12), which is complicated by the emergence of the Sunda Shelf [*Partin et al*., 2007].

[36] Shared features in the three stalagmite $\delta^{13}C$ records presented here may result from changes in rainfall amounts (via PCP) and/or the relative abundances of C_3 versus C_4 plants overlying the karst. A glacial-to-interglacial decrease of 1–2‰ in stalagmite $\delta^{13}C$ (Figure 10) is consistent with drier conditions at the research site (increased PCP), as implied by both stalagmite Mg/Ca and $\delta^{18}O$ records. On the other hand, evidence for a Sundaland "savannah corridor" [*Bird et al*., 2005] and open forest conditions [*Hunt et al*., 2012] during the LGM, implies a marked increase in the predominance of C_4 plants, providing an alternative explanation for increased stalagmite $\delta^{13}C$ during the LGM.

[37] The deglacial portion of the records (10–19 ka), are characterized by the highest variability in stalagmite Mg/Ca, Sr/Ca, and $\delta^{13}C$ over the last 27 kyr (Figures 10 and 12), perhaps related to the sequence of abrupt climate changes that occurred during this period [*Bond et al*., 1993; *Dansgaard et al*., 1993]. While, the Mg/Ca, Sr/Ca and $\delta^{13}C$ records do not contain prominent millennial-scale variability as observed in stalagmite $\delta^{18}O$, many of the centennial-scale events have analogues in the $\delta^{18}O$ records (Figure 12 and Tables 3–5). However, the relative magnitudes of the centennial-scale events in the Mg/Ca and Sr/Ca records are greater than those in the $\delta^{18}O$ records, suggesting a higher sensitivity to centennial-scale hydrological variability. In fact, the largest amplitude shifts of Mg/Ca and Sr/Ca in SCH02 and SSC01 occur in conjunction with a broad millennial-scale change in the $\delta^{18}O$ record surrounding Heinrich event 1.

6. Conclusions

[38] Spatial and temporal data sets of dripwaters from Gunung Mulu and Gunung Buda National Parks in Malaysia Borneo yield insights into the relationships between climate and geochemical karst processes in a rainforest environment. Borneo is a unique location in that it has little seasonality in temperature or rainfall, with exceptionally

high annual rainfall. We observe an inverse relationship between Mg[Sr]/Ca variability and $\delta^{18}O$ variability in dripwaters highlighting a positive correlation between residence time and mixing at our site, such that high Mg[Sr]/Ca coincides with mean rainfall $\delta^{18}O$. We uncover relatively weak signatures of PCP on Borneo dripwaters, suggesting that other processes (changes in epikarst mixing, transit pathway) exert a greater influence on dripwater Mg[Sr]/Ca values.

[39] The three different stalagmites Mg/Ca and Sr/Ca records share little in common, apart from prominent centennial-scale variations during the deglaciation. Relatively consistent changes in stalagmite Mg/Ca and $\delta^{13}C$ records during the LGM imply relatively dry conditions during that time, supporting similar inferences drawn from heavier stalagmite $\delta^{18}O$ during the LGM. Our work suggests that stalagmite $\delta^{18}O$ is the most robust paleoclimate proxy in northern Borneo stalagmites, given its high level of reproducibility. Most importantly, our study highlights the importance of reconstructing geochemical and/or isotopic variability across multiple stalagmites in order to obtain robust paleoclimate reconstructions.

Acknowledgments

[40] The authors wish to thank the staff at Gunung Mulu National Park, especially Jenny Malang and Syria Lejau, who collected the time series of cave dripwaters. We also thank Joseph Gau and Sue Clark of Gunung Mulu National Park, and Johnny Baei Hassan of Logan Bunut National Park. Joel Despain, George Prest, Shane Fryer, Jed Mosenfelder, and Brad Hacker provided field assistance during the 2003 field trip to Gunung Buda National Park. Joel Despain, Jean Krejca, Vivian Loftin, Pat Kambesis, and Alan Cressler provided field assistance during the 2006 field trip to Gunung Mulu and Gunung Buda. Nele Meckler and Stacy Carolin provided field assistance during the 2008 field trip to Gunung Mulu. Diego Fernandez provided assistance in the geochemical measurements of dripwaters from the 2003 field trip, while Matt Johnson and Nitya Sharma provided assistance with all other dripwater geochemical measurements. The authors thank two anonymous reviewers for very helpful comments. Funding for this work was provided by NSF-ATM award 0645291 to KMC and NSF-AGS award 0903099 to JFA.

References

Asrat, A., A. Baker, M. U. Mohammed, M. J. Leng, P. Van Calsteren, and C. Smith (2007), A high-resolution multiproxy stalagmite record from Mechara, Southeastern Ethiopia: Palaeohydrological implications for speleothem palaeoclimate reconstruction, *J. Quat. Sci.*, *22*(1), 53–63.

Ayalon, A., M. Bar-Matthews, and A. Kaufman (1999), Petrography, strontium, barium and uranium concentrations, and strontium and uranium isotope ratios in speleothems as palaeoclimatic proxies: Soreq Cave, Israel, *Holocene*, *9*(6), 715–722.

Baldini, J. U. L., F. McDermott, and I. J. Fairchild (2006), Spatial variability in cave drip water hydrochemistry: Implications for stalagmite paleoclimate records, *Chem. Geol.*, *235*(3-4), 390–404.

Baldini, J. U. L., F. McDermott, D. L. Hoffmann, D. A. Richards, and N. Clipson (2008), Very high-frequency and seasonal cave atmosphere P-CO2 variability: Implications for stalagmite growth and oxygen isotope-based paleoclimate records, *Earth Planet. Sci. Lett.*, *272*(1-2), 118–129.

Bar-Matthews, M., A. Ayalon, and A. Kaufman (1997), Late quaternary paleoclimate in the eastern Mediterranean region from stable isotope analysis of speleothems at Soreq Cave, Israel, *Quat. Res.*, *47*(2), 155–168.

Bar-Matthews, M., A. Ayalon, A. Kaufman, and G. J. Wasserburg (1999), The Eastern Mediterranean paleoclimate as a reflection of regional events: Soreq cave, Israel, *Earth Planet. Sci. Lett.*, *166*(1-2), 85–95.

Banner, J. L., A. Guilfoyle, E. W. James, L. A. Stern, and M. Musgrove (2007), Seasonal variations in modern speleothem calcite growth in Central Texas, USA, *J. Sedimen. Res.* *77*(7-8), 615–622.

Bird, M. I., D. Taylor, and C. Hunt (2005), Environments of insular Southeast Asia during the Last Glacial Period: A savanna corridor in Sundaland?, *Quat. Sci. Rev.*, *24*(20-21), 2228–2242.

Boch, R., C. Spotl, and S. Frisia (2011), Origin and palaeoenvironmental significance of lamination in stalagmites from Katerloch Cave, Austria, *Sedimentology*, *58*(2), 508–531.

Bond, G., W. Broecker, S. Johnsen, J. McManus, L. Labeyrie, J. Jouzel and G. Bonani (1993), Correlations between climate records from North-Atlantic sediments and Greenland ice, *Nature*, *365*(6442), 143–147.

Bradley, C., A. Baker, C. N. Jex, and M. J. Leng (2010), Hydrological uncertainties in the modelling of cave drip-water delta(18)O and the implications for stalagmite palaeoclimate reconstructions, *Quat. Sci. Rev. 29*(17-18), 2201–2214.

Burns, S. J., D. Fleitmann, A. Matter, J. Kramers, and A. A. Al-Subbary (2003), Indian Ocean climate and an absolute chronology over Dansgaard/Oeschger events 9 to 13, *Science*, *301*(5638), 1365–1367.

Cheng, H., R. L. Edwards, W. S. Broecker, G. H. Denton, X. G. Kong, Y. J. Wang, R. Zhang, and X. F. Wang (2009), Ice age terminations, *Science*, *326*(5950), 248–252.

Cobb, K. M., J. F. Adkins, J. W. Partin, and B. Clark (2007), Regional-scale climate influences on temporal variations of rainwater and cave dripwater oxygen isotopes in northern Borneo, *Earth Planet. Sci. Lett.*, *263*(3-4), 207–220.

Cosford, J., H. R. Qing, D. Mattey, B. Eglington, and M. L. Zhang (2009), Climatic and local effects on stalagmite delta(13)C values at Lianhua Cave, China, *Palaeogeogr. Palaeoclimatol. Palaeoecol.*, *280*(1-2), 235–244.

Cruz, F. W., S. J. Burns, I. Karmann, W. D. Sharp, M. Vuille, A. O. Cardoso, J. A. Ferrari, P. L. S. Dias, and O. Viana (2005), Insolation-driven changes in atmospheric circulation over the past 116,000 years in subtropical Brazil, *Nature*, *434*(7029), 63–66.

Cruz, F. W., S. J. Burns, I. Karmann, W. D. Sharp, M. Vuille, and J. A. Ferrari (2006), A stalagmite record of changes in atmospheric circulation and soil processes in the Brazilian

subtropics during the Late Pleistocene, *Quat. Sci. Rev.*, *25*(21-22), 2749–2761.

Cruz, F. W., S. J. Burns, M. Jercinovic, I. Karmann, W. D. Sharp, and M. Vuille (2007), Evidence of rainfall variations in Southern Brazil from trace element ratios (Mg/Ca and Sr/Ca) in a Late Pleistocene stalagmite, *Geochim. Cosmochim. Acta*, *71*(9), 2250–2263.

Cruz, F. W., M. Vuille, S. J. Burns, X. F. Wang, H. Cheng, M. Werner, R. L. Edwards, I. Karmann, A. S. Auler, and H. Nguyen (2009), Orbitally driven east-west antiphasing of South American precipitation, *Nat. Geosci.*, *2*(3), 210–214.

Dansgaard, W. (1964), Stable isotopes in precipitation, *Tellus*, *16*(4), 436–468.

Dansgaard, W., et al. (1993), Evidence for general instability of past climate from a 250-Kyr ice-core record, *Nature*, *364*(6434), 218–220.

Despain, J., et al. (2003), *Caves of Gunung Buda 2000*, Gunung Buda Proj. of the Natl. Speleol. Soc., Three Rivers, Calif.

Dorale, J. A., R. L. Edwards, E. Ito, and L. A. Gonzalez (1998), Climate and vegetation history of the midcontinent from 75 to 25 ka: A speleothem record from Crevice Cave, Missouri, USA, *Science*, *282*(5395), 1871–1874.

Drysdale, R. N., G. Zanchetta, J. C. Hellstrom, A. E. Fallick, J. X. Zhao, I. Isola, and G. Bruschi (2004), Palaeoclimatic implications of the growth history and stable isotope (delta O-18 and delta C-13) geochemistry of a Middle to Late Pleistocene stalagmite from central-western Italy, *Earth Planet. Sci. Lett.*, *227*(3-4), 215–229.

Fairchild, I. J., A. Borsato, A. F. Tooth, S. Frisia, C. J. Hawkesworth, Y. M. Huang, F. McDermott, and B. Spiro (2000), Controls on trace element (Sr-Mg) compositions of carbonate cave waters: Implications for speleothem climatic records, *Chem. Geol.*, *166*(3-4), 255–269.

Fairchild, I. J., A. Baker, A. Borsato, S. Frisia, R. W. Hinton, F. McDermott, and A. F. Tooth (2001), Annual to subannual resolution of multiple trace-element trends in speleothems, *J. Geol. Soc.*, *158* 831–841.

Fairchild, I. J., C. L. Smith, A. Baker, L. Fuller, C. Spotl, D. Mattey, and F. McDermott (2006a), Modification and preservation of environmental signals in speleothems, *Earth Sci. Rev.*, *75*(1-4), 105–153.

Fairchild, I. J., G. W. Tuckwell, A. Baker, and A. F. Tooth (2006b), Modelling of dripwater hydrology and hydrogeochemistry in a weakly karstified aquifer (Bath, UK): Implications for climate change studies, *J. Hydrol.*, *321*(1-4), 213–231.

Farrant, A. R., and P. L. Smart (2011), Role of sediment in speleogenesis; sedimentation and paragenesis, *Geomorphology*, *134*(1-2), 79–93.

Farrant, A. R., P. L. Smart, F. F. Whitaker, and D. H. Tarling (1995), Long-term quaternary uplift rates inferred from Limestone Caves in Sarawak, Malaysia, *Geology*, *23*(4), 357–360.

Fleitmann, D., S. J. Burns, M. Mudelsee, U. Neff, J. Kramers, A. Mangini, and A. Matter (2003), Holocene forcing of the Indian monsoon recorded in a stalagmite from Southern Oman, *Science*, *300*(5626), 1737–1739.

Fleitmann, D., et al. (2007), Holocene ITCZ and Indian monsoon dynamics recorded in stalagmites from Oman and Yemen (Socotra), *Quat. Sci. Rev.*, *26*(1-2), 170–188.

Fleitmann, D., et al. (2009), Timing and climatic impact of Greenland interstadials recorded in stalagmites from northern Turkey, *Geophys. Res. Lett.*, *36*, L19707, doi:10.1029/2009GL040050.

Frappier, A., D. Sahagian, L. A. Gonzalez, and S. J. Carpenter (2002), El Nino events recorded by stalagmite carbon isotopes, *Science*, *298*(5593), 565–565.

Frisia, S., I. J. Fairchild, J. Fohlmeister, R. Miorandi, C. Spotl, and A. Borsato (2011), Carbon mass-balance modelling and carbon isotope exchange processes in dynamic caves, *Geochim. Cosmochim. Acta*, *75*(2), 380–400.

Fuller, L., A. Baker, I. J. Fairchild, C. Spotl, A. Marca-Bell, P. Rowe, and P. F. Dennis (2008), Isotope hydrology of dripwaters in a Scottish cave and implications for stalagmite palaeoclimate research, *Hydrol. Earth Syst. Sci. 12*(4), 1065–1074.

Galy, A., M. Bar-Matthews, L. Halicz, and R. K. O'Nions (2002), Mg isotopic composition of carbonate: Insight from speleothem formation, *Earth Planet. Sci. Lett.*, *201*(1), 105–115.

Genty, D., A. Baker, M. Massault, C. Proctor, M. Gilmour, E. Pons-Branchu, and B. Hamelin (2001), Dead carbon in stalagmites: Carbonate bedrock paleodissolution vs. ageing of soil organic matter. Implications for C-13 variations in speleothems, *Geochim. Cosmochim. Acta*, *65*(20), 3443–3457.

Genty, D., D. Blamart, R. Ouahdi, M. Gilmour, A. Baker, J. Jouzel, and S. Van-Exter (2003), Precise dating of Dansgaard-Oeschger climate oscillations in western Europe from stalagmite data, *Nature*, *421*(6925), 833–837.

Genty, D., D. Blamart, B. Ghaleb, V. Plagnes, C. Causse, M. Bakalowicz, K. Zouari, N. Chkir, J. Hellstrom, K. Wainer, and F. Bourges (2006), Timing and dynamics of the last deglaciation from European and North African delta C-13 stalagmite profiles—Comparison with Chinese and South Hemisphere stalagmites, *Quat. Sci. Rev.*, *25*(17-18), 2118–2142.

Gokturk, O. M., D. Fleitmann, S. Badertscher, H. Cheng, R. L. Edwards, M. Leuenberger, A. Fankhauser, O. Tuysuz, and J. Kramers (2011), Climate on the southern Black Sea coast during the Holocene: Implications from the Sofular Cave record, *Quat. Sci. Rev.*, *30*(19-20), 2433–2445.

Griffiths, M. L., et al. (2009), Increasing Australian-Indonesian monsoon rainfall linked to early Holocene sea-level rise, *Nat. Geosci.*, *2*(9), 636–639.

Hellstrom, J., M. McCulloch, and J. Stone (1998), A detailed 31,000-year record of climate and vegetation change, from the isotope geochemistry of two New Zealand speleothems, *Quat. Res.*, *50*(2), 167–178.

Hendy, C. H. (1971), Isotopic geochemistry of speleothems, 1. Calculation of effects of different modes of formation on isotopic composition of speleothems and their applicability as palaeoclimatic indicators, *Geochim. Cosmochim. Acta*, *35*(8), 801–824.

Holmgren, K., J. A. Lee-Thorp, G. R. J. Cooper, K. Lundblad, T. C. Partridge, L. Scott, R. Sithaldeen, A. S. Talma, and P. D. Tyson (2003), Persistent millennial-scale climatic variability over the past 25,000 years in Southern Africa, *Quat. Sci. Rev.*, *22*(21-22), 2311–2326.

Huang, H. M., I. J. Fairchild, A. Borsato, S. Frisia, N. J. Cassidy, F. McDermott, and C. J. Hawkesworth (2001), Seasonal variations in Sr, Mg and P in modern speleothems (Grotta di Ernesto, Italy), *Chem. Geol.*, *175*(3-4), 429–448.

Huang, Y. M., and I. J. Fairchild (2001), Partitioning of Sr2+ and Mg2+ into calcite under karst-analogue experimental conditions, *Geochim. Cosmochim. Acta*, *65*(1), 47–62.

Hunt, C. O., D. D. Gilbertson, and G. Rushworth (2012), A 50,000-year record of late Pleistocene tropical vegetation and human impact in lowland Borneo, *Quat. Sci. Rev.*, *37* 61–80.

Ihlenfeld, C., M. D. Norman, M. K. Gagan, R. N. Drysdale, R. Maas, and J. Webb (2003), Climatic significance of seasonal trace element and stable isotope variations in a modern freshwater tufa, *Geochim. Cosmochim. Acta*, *67*(13), 2341–2357.

Johnson, K. R., C. Y. Hu, N. S. Belshaw, and G. M. Henderson (2006), Seasonal trace-element and stable-isotope variations in a Chinese speleothem: The potential for high-resolution paleomonsoon reconstruction, *Earth Planet. Sci. Lett.*, *244*(1-2), 394–407.

Jex, C. N., A. Baker, I. J. Fairchild, W. J. Eastwood, M. J. Leng, H. J. Sloane, L. Thomas, and E. Bekaroglu (2010), Calibration of speleothem delta(18)O with instrumental climate records from Turkey, *Global Planet. Chan. 71*(3-4), 207–217.

Lambert, W. J., and P. Aharon (2011), Controls on dissolved inorganic carbon and delta(13)C in cave waters from DeSoto Caverns: Implications for speleothem delta(13)C assessments, *Geochim. Cosmochim. Acta*, *75*(3), 753–768.

Lorens, R. B. (1981), Sr, Cd, Mn, and Co distribution coefficients in calcite as a function of calcite precipitation rate, *Geochim. Cosmochim. Acta*, *45*(4), 553–561.

Lorrey, A., P. Williams, J. Salinger, T. Martin, J. Palmer, A. Fowler, J. X. Zhao, and H. Neil (2008), Speleothem stable isotope records interpreted within a multi-proxy framework and implications for New Zealand palaeoclimate reconstruction, *Quat. Internat. 187*, 52–75.

Madden, R. A., and P. R. Julian (1971), Detection of a 40–50 day oscillation in zonal wind in tropical Pacific, *J. Atmos. Sci.*, *28*(5), 702–708.

Mattey, D., D. Lowry, J. Duffet, R. Fisher, E. Hodge, and S. Frisia (2008), A 53 year seasonally resolved oxygen and carbon isotope record from a modem Gibraltar speleothem: Reconstructed drip water and relationship to local precipitation, *Earth Planet. Sci. Lett.*, *269*(1-2), 80–95.

McDermott, F. (2004), Palaeo-climate reconstruction from stable isotope variations in speleothems: A review, *Quat. Sci. Rev.*, *23*(7-8), 901–918.

McDonald, J., R. Drysdale, and D. Hill (2004), The 2002–2003 El Nino recorded in Australian cave drip waters: Implications for reconstructing rainfall histories using stalagmites, *Geophys. Res. Lett.*, *31*, L22202, doi:10.1029/2004GL020859.

McMillan, E. A., I. J. Fairchild, S. Frisia, A. Borsato, and F. McDermott (2005), Annual trace element cycles in calcite-aragonite speleothems: Evidence of drought in the western Mediterranean 1200-1100 yr BP, *J. Quat. Sci.*, *20*(5), 423–433.

Meyer, M. C., R. Faber, and C. Spotl (2006), The WinGeol Lamination Tool: New software for rapid, semi-automated analysis of laminated climate archives, *Holocene*, *16*(5), 753–761.

Mickler, P. J., J. L. Banner, L. Stern, Y. Asmerom, R. L. Edwards, and E. Ito (2004), Stable isotope variations in modern tropical speleothems: Evaluating equilibrium vs. kinetic isotope effects, *Geochim. Cosmochim. Acta*, *68*(21), 4381–4393.

Moerman, J. W., K. M. Cobb, J. F. Adkins, H. Sodemann, B. Clark, and A. A. Tuen (2013), Large-scale controls on diurnal to interannual rainfall oxygen isotopic variability in the West Pacific Warm Pool, *Earth Planet. Sci. Lett.*, doi:2010.1016/J.EPSL.2013.2003.2014, in press.

Musgrove, M., and J. L. Banner (2004), Controls on the spatial and temporal variability of vadose dripwater geochemistry: Edwards Aquifer, central Texas, *Geochim. Cosmochim. Acta*, *68*(5), 1007–1020.

Oster, J. L., I. P. Montanez, T. P. Guilderson, W. D. Sharp, and J. L. Banner (2010), Modeling speleothem delta(13)C variability in a central Sierra Nevada cave using (14)C and (87)Sr/(86)Sr, *Geochim. Cosmochim. Acta*, *74*(18), 5228–5242.

Paquette, J., and R. J. Reeder (1995), Relationship between surface-structure, growth-mechanism, and trace element incorporation into calcite, *Geochim. Cosmochim. Acta*, *59*(4), 735–749.

Partin, J. W., K. M. Cobb, J. F. Adkins, B. Clark, and D. P. Fernandez (2007), Millennial-scale trends in Warm Pool hydrology since the Last Glacial Maximum, *Nature*, *449*(7161), 452–455.

Partin, J. W., et al. (2012), Relationship between modern rainfall variability, cave dripwater, and stalagmite geochemistry in Guam, USA, *Geochem. Geophys. Geosyst.*, *13*, Q03013, doi:10.1029/2011GC003930.

Roberts, M. S., P. L. Smart, and A. Baker (1998), Annual trace element variations in a Holocene speleothem, *Earth Planet. Sci. Lett.*, *154*(1-4), 237–246.

Rozanski, K., L. Araguas-Araguas, and R. Gonfiantini (1993), Isotopic patterns in modern global precipitation, in *Climate Change in Continental Isotopic Records*, edited by P. K. Swart, et al., pp. 1–36, AGU, Washington, D. C.

Rudzka, D., F. McDermott, L. M. Baldini, D. Fleitmann, A. Moreno, and H. Stoll (2011), The coupled delta(13)C-radiocarbon systematics of three Late Glacial/early Holocene speleothems; insights into soil and cave processes at climatic transitions, *Geochim. Cosmochim. Acta*, *75*(15), 4321–4339.

Schimpf, D., R. Kilian, A. Kronz, K. Simon, C. Spotl, G. Worner, M. Deininger, and A. Mangini (2011), The significance of chemical, isotopic, and detrital components in three coeval stalagmites from the superhumid southernmost Andes (53 degrees S) as high-resolution palaeo-climate proxies, *Quat. Sci. Rev. 30*(3-4), 443–459.

Schrag, D. P. (1999), Rapid analysis of high-precision Sr/Ca ratios in corals and other marine carbonates, *Paleoceanography*, *14*(2), 97–102.

Sinclair, D. J. (2011), Two mathematical models of Mg and Sr partitioning into solution during incongruent calcite dissolution Implications for dripwater and speleothem studies, *Chem. Geol.*, *283*(3-4), 119–133.

Sinclair, D. J., J. L. Banner, F. W. Taylor, J. Partin, J. Jenson, J. Mylroie, E. Goddard, T. Quinn, J. Jocson, and B. Miklavic (2012), Magnesium and strontium systematics in tropical speleothems from the Western Pacific, *Chem. Geol.*, *294*, 1–17.

Spotl, C., I. J. Fairchild, and A. F. Tooth (2005), Cave air control on dripwater geochemistry, Obir Caves (Austria): Implications for speleothem deposition in dynamically ventilated caves, *Geochim. Cosmochim. Acta*, *69*(10), 2451–2468.

Tooth, A. F., and I. J. Fairchild (2003), Soil and karst aquifer hydrological controls on the geochemical evolution of speleothem-forming drip waters, Crag Cave, southwest Ireland, *J. Hydrol.*, *273*(1-4), 51–68.

Treble, P., J. M. G. Shelley, and J. Chappell (2003), Comparison of high resolution sub-annual records of trace elements in a modern (1911–1992) speleothem with instrumental climate data from southwest Australia, *Earth Planet. Sci. Lett.*, *216*(1-2), 141–153.

Treble, P. C., J. Chappell, and J. M. G. Shelley (2005), Complex speleothem growth processes revealed by trace element

mapping and scanning electron microscopy of annual layers, *Geochim. Cosmochim. Acta*, *69*(20), 4855–4863.

Tremaine, D. M., P. N. Froelich, and Y. Wang (2011), Speleothem calcite farmed in situ: Modern calibration of delta(18)O and delta(13)C paleoclimate proxies in a continuously-monitored natural cave system, *Geochim. Cosmochim. Acta*, *75*(17), 4929–4950.

Waltham, A. C., and D. B. Brook (1980), Symposium on the geomorphology of the Mulu Hills.8. Cave development in the Melinau limestone of the Gunung-Mulu National-Park, *Geogr. J.*, *146*, 258–266.

Wang, X., A. S. Auler, R. L. Edwards, H. Cheng, E. Ito, and M. Solheid (2006), Interhemispheric anti-phasing of rainfall during the last glacial period, *Quat. Sci. Rev.*, *25*(23-24), 3391–3403.

Wang, Y. J., H. Cheng, R. L. Edwards, Z. S. An, J. Y. Wu, C. C. Shen, and J. A. Dorale (2001), A high-resolution absolute-dated Late Pleistocene monsoon record from Hulu Cave, China, *Science*, *294*(5550), 2345–2348.

Wannier, M. (2009), Carbonate platforms in wedge-top basins: An example from the Gunung Mulu National Park, Northern Sarawak (Malaysia), *Mar. Petrol. Geol.*, *26*(2), 177–207.

Williams, P. W., D. N. T. King, J. X. Zhao, and K. D. Collerson (2005), Late pleistocene to holocene composite speleothem O-18 and C-13 chronologies from south island, new Zealand-did a global younger dryas really exist? *Earth Planet. Sci. Lett.*, *230*(3-4), 301–317.

Zhang, C. D. (2005), Madden-Julian oscillation, *Rev. Geophys.*, *43*, RG2003, doi:10.1029/2004RG000158.